Report 3182

NAVAL SHIP RESEARCH AND DEVELOPMENT CENTER

Washington, D.C. 20007

STATIC STRESSES ON WIDE-BLADED PROPELLERS

DEPARTMENT OF HYDROMECHANICS

RESEARCH AND DEVELOPMENT REPORT

February 1970

Report 3182

STATIC STRESSES ON WIDE-BLADED PROPELLERS

The Naval Ship Research and Development Center is a U.S. Navy center for laboratory effort directed at achieving improved sea and air vehicles. It was formed in March 1967 by merging the David Taylor Model Basin at Carderock, Maryland and the Marine Engineering Laboratory at Annapolis, Maryland. The Mine Defense Laboratory, Panama City, Florida became part of the Center in November 1967.

Naval Ship Research and Development Center
Washington, D.C. 20007

DEPARTMENT OF THE NAVY
NAVAL SHIP RESEARCH AND DEVELOPMENT CENTER
WASHINGTON, D. C. 20007

STATIC STRESSES ON WIDE-BLADED PROPELLERS

by

J.H. McCarthy and
J.S. Brock

February 1970 Report 3182

TABLE OF CONTENTS

LIST OF FIGURES

LIST OF TABLES

ABSTRACT

Static stresses were obtained in laboratory experiments for a destroyer propeller, having aerofoil blade sections, and a supercavitating propeller, having wedge-shaped blade sections, using specially constructed pressure chambers that allowed the blade faces to be loaded under air pressure. A new method for applying beam theory is presented that closely predicts the magnitude and distribution of radial stresses on the destroyer propeller blade. For the supercavitating propeller, neither the proposed beam-theory method nor a particular computerized-shell analysis can be considered entirely satisfactory for prediction of blade stresses.

ADMINISTRATIVE INFORMATION

The experiments described in this paper were carried out from 1962 to 1964 at the David Taylor Model Basin (now the Naval Ship Research and Development Center) and were sponsored by the Bureau of Ships with funding under Subproject S-R009 01 01, Task 103.

INTRODUCTION

The reported study was undertaken to determine the adequacy of beam and/or shell theories for predicting static-stress distribution on the blades of highly pitched, wide-bladed propellers. Two nonskewed, nonraked, model-sized propellers were selected for laboratory investigation and were subjected to uniform air-pressure loading over either all or part of their blade faces. One was a destroyer propeller, having aerofoil blade sections; the other was a supercavitating propeller, having wedge-shaped blade sections. Except for the type of blade section, the destroyer propeller studied was geometrically much like that tested earlier by Conolly.[1] At the time of the described tests, no previous stress experiments had been reported for supercavitating propellers. Since then, Morita[2] and Davis and English[3] have published laboratory stress data for wedge-shaped blade sections.

---

[1]References are listed on page 29.

Apart from the work of Conolly,[1] Terletsky,[4] and Antonides,[5] past laboratory and shipboard measurements of stresses on propellers, having conventional aerofoil or segmental sections, have been confined to moderately pitched, narrow-bladed propellers. No one considered extremely skewed blades. All but one of the studies seems to have been done in the Netherlands--Rosingh,[6] Biezeno,[7] Romson,[8] and Wereldsma.[9] All were carried out from 1944 to 1965. The remaining stress work, which included both laboratory and shipboard measurements, was done by the Shipbuilding Research Association of Japan.[10] In some of the laboratory tests that have been undertaken, the propeller blades were statically loaded by a succession of discrete forces, e.g., Morita, Biezeno. The Conolly propeller was loaded by forcing a blade face against a pad of "silicone bouncing putty" which was in contact with a fixed block having a helicoidal surface. Davis and English, Terletsky, and Wereldsma loaded their propellers through actual testing in a water tunnel. Table 1 gives a partial summary of the particulars for the previously described work and the present study.

The traditional approach to calculating propeller blade stress has been to consider a blade as a cantilever attached to the propeller hub and to apply the simple bending theory of beams. Using such an approach, only radial stresses have been evaluated. For a given radial distribution of blade loading, the usual method of applying beam theory has been credited to Taylor,[11] who recommended that stresses be calculated for cylindrical blade sections with neutral axes selected parallel and perpendicular to the (straight) nose-to-tail (pitch) line of the expanded view of the section. The method was later criticized by Rosingh[12] and Hancock;[13] Rosingh proposed that stress calculations should be performed for plane rather than cylindrical sections. In either case, however, because of the choice of neutral axes, the magnitudes of calculated stresses at the blade leading and trailing edges tend to be relatively high for cambered sections.

Experimentally, for cambered aerofoil and segmental sections, Biezeno, Conolly, and Terletsky found that the measured stresses were maximum near the point of maximum section thickness and tended to fall off near the leading and trailing edges, with corresponding face and back stresses nearly equal and opposite. If one assumes a linear variation of stress across the blade section, the latter finding indicates that the

chordwise neutral axis roughly follows the midthickness line of the blade section, rather than being parallel to the nose-tail line. (Use will be made of this observation later in carrying out beam theory calculations.) However, for wedge-shaped blade sections, the experiments of Morita and Davis and English gave no such simple picture, indicating that maximum principle stresses occurred near the quarter-chord line and were greatest at approximately 70 percent of the propeller radius. For such blades the conventional beam theory was clearly not adequate.

Despite the different ways in which beam theory has been applied and the discrepancies between calculated and measured stress distributions for moderately pitched, narrow-bladed propellers having conventional sections, it is generally believed that some form of beam theory will give adequate predictions of maximum stress. Cohen,[14] in a treatise on shell theory, remarked that maximum stresses calculated by the Taylor and Rosingh methods agreed equally well with experimental results by Biezeno. For engineering calculations Cohen recommends the Taylor method which is slightly more conservative and more straightforward than the Rosingh method. For narrow blades he found the Rosingh method to be more accurate; for wide blades, less accurate. Further, on the basis of shipboard measurements of stresses near the root section of a tanker propeller, Wereldsma[9] found that the average maximum stresses predicted by various forms of beam theory were conservative.

For wide-bladed propellers it has been conjectured that beam theory is inadequate for evaluating stress, and a method of calculation based on shell theory is required; see Reference 15. Unlike the beam theory, shell theory could allow for the effects of blade curvature and nonuniform chordwise load distributions and could lead to predictions of principal stresses. The first attempted application of shell theory to propellers was apparently by Cohen,[14] who, following a number of approximations, concluded by recommending use of the Taylor version of beam theory. Later, Conolly[1] presented a simplified shell analysis that gave predictions of the magnitude and distribution of radial and transverse blade stresses that were in generally good agreement with laboratory and shipboard measurements of destroyer propeller stresses. Beam-theory calculations were not included in the Conolly work. In 1964, Lieberman[16] developed an

elaborate computer program, based on a shell analysis by Lane,[17] which made fewer approximations and permitted calculation of propeller blade-static stresses and deflections as well as blade-vibration natural frequencies, mode shapes, and stress distributions. Static-stress calculations for wide-bladed propellers used approximately 100 minutes of IBM-7090 computer running time. The major problem in using the program appears to be the size limitations of existing computer equipment in allowing a fine enough mesh for adequate representation of propeller geometry. Static stress predictions by the program will be compared with measured stresses later.

Before concluding the section, it is important to emphasize that the preceding discussion, and all that follows, is concerned only with propeller stress under steady loading. A shipboard propeller in operation will experience cyclic stressing due to nonuniform inflow to the propeller, high-transient loading during ship maneuvers, and in some cases significant vibration stresses due to excitation at or near blade natural frequencies. A structurally adequate propeller-design procedure must take into consideration such unsteady stressing, and a fatigue analysis should be included. The reason for concentrating attention on blade stress under steady loading is that adequate knowledge may provide a basis for making quasi-steady engineering estimates of the nonvibratory unsteady stresses in propeller blades.

DESCRIPTION OF EXPERIMENTS

Laboratory strain measurements were carried out on two stainless steel model-sized propellers--a four-bladed 16-inch-diameter destroyer propeller (Figure 1), having aerofoil blade sections, and a three-bladed 18-inch-diameter supercavitating propeller (Figure 2), having wedge-shaped blade sections. Offsets for the propellers are given in the Appendix. Both propellers are nonraked and nonskewed with highly pitched, wide blades with an aspect ratio that is near to unity (based on mean chord length). The maximum chord length of the destroyer propeller blade occurs at 60 percent of the tip radius. Maximum section thickness occurs near midchord. For the supercavitating propeller, the maximum chord length occurs at the hub and remains about the same to 60 percent of the tip

radius. The blade is very highly pitched, with a consequent extreme twist of the blade sections. Maximum section thickness occurs at or near the trailing edge.

For each propeller, a pressure chamber was constructed to fit around one blade to allow face loading under uniform air pressure. The pressure chamber was made from a wooden block in two halves, which, when fitted togehter, had cutouts conforming to the projected blade outline and the propeller hub outline; see Figure 3. A plastic wood filler (Araldite) was used in the hub area to assure a tight fit when the mating blocks were assembled around the propeller. The blade-outline cutout was oversized to allow approximately 0.010-inch clearance between the blocks and the edge of the propeller blade. The top and bottom of the block-propeller assembly were fitted with gasketed 3/8-inch-thick steel plates, and the entire rig was held together by vertical bolts between the top and bottom plates. A large bolt was also fitted through the hub, and dowel pins were provided between the hub and plates to prevent rigid body rotation of the propeller blade and consequent contact with the wooden blocks during pressure loading.

The volume bounded by the blade face, propeller hub, wooden blocks, and top plate comprised the pressure chamber. The top plate was provided with three holes for an air supply, a pressure gage, and a stuffing tube for exit of strain gage wires attached to the blade face; see Figure 4. The bottom plate had a cutout conforming to the projected blade outline, from which strain gage wires attached to the blade back exited; see Figure 5. The opening also provided access for inspection of blade-block clearances during pressure loading. During all tests, clearances were monitored both visually and by use of feeler gages. In some of the tests, local contact, due to large blade deflection under high pressure, was noticed; clearances were subsequently increased locally by removing wood.

To prevent excessive air leakage from the pressure chamber through the gap between the blade edge and the wooden blocks, a rubber O-ring, one-eighth of an inch in diameter, was laid along the gap around the entire blade outline. To hold the O-ring in place, a soft putty (Plasticine) was smeared over it, forming a fillet between the edge of the blade face and the adjacent wooden blocks. During most of the testing,

air-leakage rates for a given pressure loading were monitored by a flowmeter attached to the air supply line. At low air pressures, leakage was nil. Occasionally at the higher pressures employed (up to 40 psi) leakage rates would abruptly increase. Such leaks were usually distinctly audible and could be located by feeling around with the hand. In such cases readjustment of the O-ring, tightening of bolts, and judicious application of putty to the pressure rig would usually correct the situation.

In addition to the tests on both propellers when uniform pressure was applied over the entire blade face, experiments were performed on the destroyer propeller to determine the effect of nonuniform-chordwise pressure distribution on blade stress. The test was accomplished by using a curved vertical plate welded to the bottom side of the top cover plate, which divided the pressure chamber into two compartments. The divider plate, which intersected the blade along its forward quarter-chord line, had a knife-edge that cleared the blade face by approximately 0.010 inch. Air leakage from one compartment to another was minimized by further use of an O-ring and putty, laid along the side of the divider plate on which air pressure was to be applied. Thus, uniform pressure could be separately applied to either the forward one-quarter of the blade, simulating peak leading-edge loading, or to the after three-quarters of the blade. A measure of the reliability of stresses obtained is shown in Figure 6, where root stresses obtained without the divider plate are compared with root stresses obtained by summing the stresses from tests in which each compartment was separately pressurized.

For all of the pressure tests undertaken on the two propellers, strain gages were located at 30, 50, 70, and 90 percent of blade-tip radius. In some tests, the gages were laid along plane blade sections and in others along cylindrical blade sections, with the number of gage locations for each section being varied between four and seven, depending on the section chord length. For every strain gage located on the blade face, there was a corresponding gage on the blade back. In some tests, two stacked strain gages were placed at each location. One was directed transversely; the other, orthogonal to it. In other tests, strain rosettes were used. Budd Metalfilm Strain Gages were used throughout, either strain gage Type C6-121 or strain rosette Type C6-124R3TS.

The destroyer propeller blade was pressure loaded up to 30 psi and the supercavitating propeller blade up to 40 psi, each in 5-psi increments. For a given pressure setting, strain gage signals were graphically recorded by high-speed 48-channel Gilmore Strain Gage Plotters (Model 114, Serial 1040). Each pressure setting required about 2 minutes for the recorders to plot all strain measurements. With few exceptions, the strain versus pressure plots were linear with little or no scatter, and the results were repeatable. All experimental data presented in the next section are results of tests that have been repeated from two to four times under identical conditions. The small number of bad gages for which measurements were not repeatable or linear are not reported. Stresses were calculated from the strain measurements by the usual formulas, taking Poisson's Ratio=0.30 and Young's Modulus = $30X10^6$ psi, values appropriate for stainless steel. Figure 7 shows the stress conventions used for gages located on both plane and cylindrical blade sections. As it turned out, whenever strain rosettes were used, they were applied along cylindrical blade sections.

RESULTS AND COMPARISONS

DESTROYER PROPELLER

The first tests on the destroyer-propeller blade were under uniform pressure applied over the entire blade face, with strain gages laid along plane blade sections. Experimentally determined longitudinal and transverse stresses at four blade sections are shown in Figure 8. The stresses plotted are for a 1-psi uniform-pressure load. Near the blade root, the maximum transverse stress is about one-third of the maximum longitudinal stress, and the stresses gradually become more nearly equal in magnitude towards the blade tip. The measured stresses are maximum near the points of maximum section thickness, falling off towards the blade edges, with corresponding face and back stresses being roughly equal and opposite.

The previously described qualitative results agree with results obtained experimentally by Conolly,[1] Terletsky,[4] and Biezeno[7] as discussed in the introduction and indicate that the chordwise neutral axis roughly follows the section midthickness line. Thus, beam theory-stress

calculations* for uniform-pressure loading have been carried out, using cylindrical blade sections,[11] with neutral axes and section moduli, computed for an equivalent section having zero camber but the same thickness distribution as the actual expanded-blade section. The centerline longitudinal (radial) stresses calculated by the "equivalent-beam method" are shown in Figure 8, and the agreement with experiment is quite satisfactory.

A second uniform-pressure test was undertaken; however, strain rosettes were laid along a cylindrical blade section at 30 percent of propeller-tip radius. Figure 9 shows the experimentally determined radial and circumferential stress distributions. Also shown is the chordwise distribution of radial stress, computed according to the equivalent-beam method, which closely follows the experimental results. The good correlation shown in Figures 8 and 9 does not result from the usual application of beam theory, which predicts relatively high radial tensile stresses near both the section leading and trailing edges, and lower radial tensile stresses on the blade face at the locations of section maximum thickness.

Blade stresses under uniform-pressure loading were also calculated from the Lane[17] version of shell theory, using the computer program developed by Lieberman.[16] The program allows a choice up to 108 degrees of freedom (a measure of the fineness of representation of blade geometry) and calculates longitudinal, transverse, and shear stresses for plane blade sections. Figure 10 shows some representative longitudinal and transverse stress distributions calculated by the program for both 84 and 108 degrees of freedom, along with experimental stress results. At 84 degrees of freedom the longitudinal stresses are seriously underestimated. For 108 degrees of freedom, calculated longitudinal and transverse stress magnitudes and distributions are in fair agreement with the experimental results. Because of the large discrepancy between

*See, e.g., Equation 105 of the Schoenherr paper.[18]

stresses calculated at 84 and 108 degrees of freedom, a larger degree-of-freedom number is probably required to assure a more adequate representation of blade geometry and an accurate prediction of stresses.

The final tests performed on the destroyer propeller were designed to investigate the effect of nonuniform chordwise-load distribution on blade stress. As explained in the previous section, the test was accomplished by dividing the pressure chamber into two compartments so that the blade could be loaded either over the area extending from the blade leading edge to the quarter-chord line or over the area extending from the quarter-chord line to the blade trailing edge. Experimentally derived stresses from the tests, along with the results for uniform chordwise-pressure distribution, are shown in Figure 11 for the cylindrical blade section at 30 percent of tip radius. Strain rosettes were employed. In each case the stresses are for the same total radial load distribution, with the stresses from the uniform-pressure tests referred to a 1-psi loading. Stresses under nonuniform chordwise loading were also obtained for other radii, with results qualitatively the same as those shown in Figure 11. For loading concentrated near the blade leading edge both the circumferential and radial stresses are higher towards the leading edge and lower towards the trailing edge than are the corresponding stresses obtained under uniform pressure. For loading towards the blade trailing edge, the reverse is true. In either case the maximum blade stresses are not remarkably different from those obtained under uniform pressure and are generally within the stress curves calculated by the equivalent-beam method.

Principal stresses and directions on the blade face, calculated from the strain rosette measurements, are presented in Table 2 for each type of loading; see Figure 7 for nomenclature. In every case, save one of little consequence, the magnitudes and directions of the maximum principal stresses near the blade root closely agree with the magnitude and direction of the radial stress. Rosette measurements were not made at larger radii for the destroyer propeller.

SUPERCAVITATING PROPELLER

Two sets of tests were performed for the supercavitating propeller, both with uniform air pressure applied over the entire blade face. For

the first test, longitudinal and transverse strain gages were laid along plane blade sections; for the second test, strain rosettes were laid along cylindrical blade sections at 30, 50, 70, and 90 percent of tip radius. Experimentally determined stresses for the first and second tests are shown in Figures 12 and 13, respectively. The stresses plotted are for a 1-psi uniform-pressure load. As with the destroyer propeller, near the blade root the maximum transverse (circumferential) stress is about one-third of the maximum longitudinal (radial) stress, while near the blade tip the former is equal to or greater than the latter stress. Remarkably unlike the destroyer propeller, however, the maximum longitudinal (radial) stress near the blade root occurs close to the blade centerline rather than near the location of maximum thickness at the blade trailing edge. For increasingly larger radii the locations of maximum longitudinal (radial) stresses tend to shift toward the blade trailing edge; however, the stresses remain relatively constant from the blade centerline to trailing edge at a given blade section. Stresses fall off towards the blade leading edge; however, corresponding face and back stresses are not as nearly equal and opposite as is the case with the destroyer propeller, which has aerofoil blade sections.

The previously described qualitative observations obviously suggest that calculations obtained by the equivalent-beam method will not be proper predictions of the stress distribution for the wedge-shaped sections of the supercavitating propeller. As shown in Figure 13, the maximum radial stresses are predicted by the method to be at the locations of maximum thickness, which occur at or near the blade trailing edge. The only feature of the predicted stresses by the equivalent-beam method of calculation that closely agrees with the experimental results is the magnitude of maximum radial stress at each section. However, the good agreement may be merely fortuitous. In any event, it must be concluded that the equivalent-beam method is inadequate for the prediction of stress distribution on wide-bladed supercavitating propellers with wedge-shaped sections. The same conclusion also applies to other methods of application of beam theory that have been proposed.

Shell-theory blade stresses for uniform-pressure loading, calculated by the Lieberman[16] computer program, are shown plotted in Figure 12

for a run using 84 degrees of freedom. Calculated stresses near the blade edge, which are shown in Figure 12, are distinctly haywire. A computer run was also made at 63 degrees of freedom, with maximum stresses as much as 15 percent lower than those calculated at 84 degrees of freedom. At 108 degrees of freedom, the calculated stresses were generally haywire. In most cases the calculated maximum stresses shown in Figure 13 tend to be conservative. The calculated stress distributions, while not in good agreement with experiment, do possess some of the correct characteristics. In general, the stresses calculated at 84 degrees of freedom are more sinuous than the experimental stresses, probably indicating that a greater accuracy and/or more degrees of freedom are required to adequately represent the blade geometry.

Principal stresses and directions on the blade face and back, calculated from the strain rosette measurements, are presented in Table 3; see Figure 7 for nomenclature. Near the blade root, at 30 percent of tip radius, the magnitudes and directions of the maximum principal stresses agree closely with those for the radial stress, except near the trailing edge. At the larger radii, for which stresses are lower, the magnitude of the maximum principal stresses become as much as three times as large as the radial stresses, with directions appreciably different from radial. (The same sort of result is probably true for the destroyer-propeller blade at larger radii.)

CONCLUSIONS

BLADES WITH AEROFOIL SECTIONS

For uniform-pressure loading, static stresses on a given section are a maximum near the point of maximum section thickness, falling off towards the blade edges, with corresponding face and back stresses being nearly equal in magnitude and opposite in sign. The effect of nonuniform chordwise-pressure loading is to shift the chordwise location of maximum stress without significantly altering its magnitude. Near the blade root the maximum principal stresses closely agree with the magnitudes and directions of the radial stresses, and the maximum transverse stress is about one-third of the maximum longitudinal stress. The longitudinal

and transverse stresses become more nearly equal towards the blade tip. The equivalent-beam method, which uses cylindrical blade sections and zero camber, closely predicts the magnitude and distribution of radial stresses for aerofoil blade sections. (It is, no doubt, also adequate for blades with segmental sections, based on the experimental work of Conolly[1] and Terletsky.)[4] For 108 degrees of freedom, the Lieberman[16] shell-analysis program predicted stress distributions in fair agreement with experiment.

BLADES WITH WEDGE-SHAPED SECTIONS

For uniform pressure loading, maximum radial stresses near the blade root occur close to the blade centerline rather than near the location of maximum thickness at the trailing edge. For larger radii the radial stress remains relatively constant, at its maximum values, from the blade centerline to the trailing edge. Stresses fall off toward the leading edge; however, corresponding face and back stresses are not as nearly equal and opposite as for blades with aerofoil sections. Near the blade root the magnitude and direction of the maximum principal stresses closely agree with those for the radial stresses, except near the trailing edge. The close agreement is not true for larger radii. The radial stress distribution is not properly predicted by the equivalent-beam method at a given section; however, the magnitudes of the maximum radial stresses are closely predicted for the particular blade tested. Calculations using the Lieberman[16] shell-analysis computer program for 84 degrees of freedom gave generally conservative predictions of maximum transverse and longitudinal stresses but only fair stress distributions. The program should be further developed to provide greater reliability, accuracy, and/or more degrees of freedom so that complex blade geometries may be adequately represented.

ACKNOWLEDGMENTS

The authors are particularly grateful to the late Charles D. Bradfield, who was responsible for the emplacement of strain gages and associated wiring. The first-named author is responsible for the analyses and text presented here, and takes full responsibility for any of their shortcomings. The experimental part of the study was a joint effort, but primary credit for perfection of the test technique belongs to the second-named author.

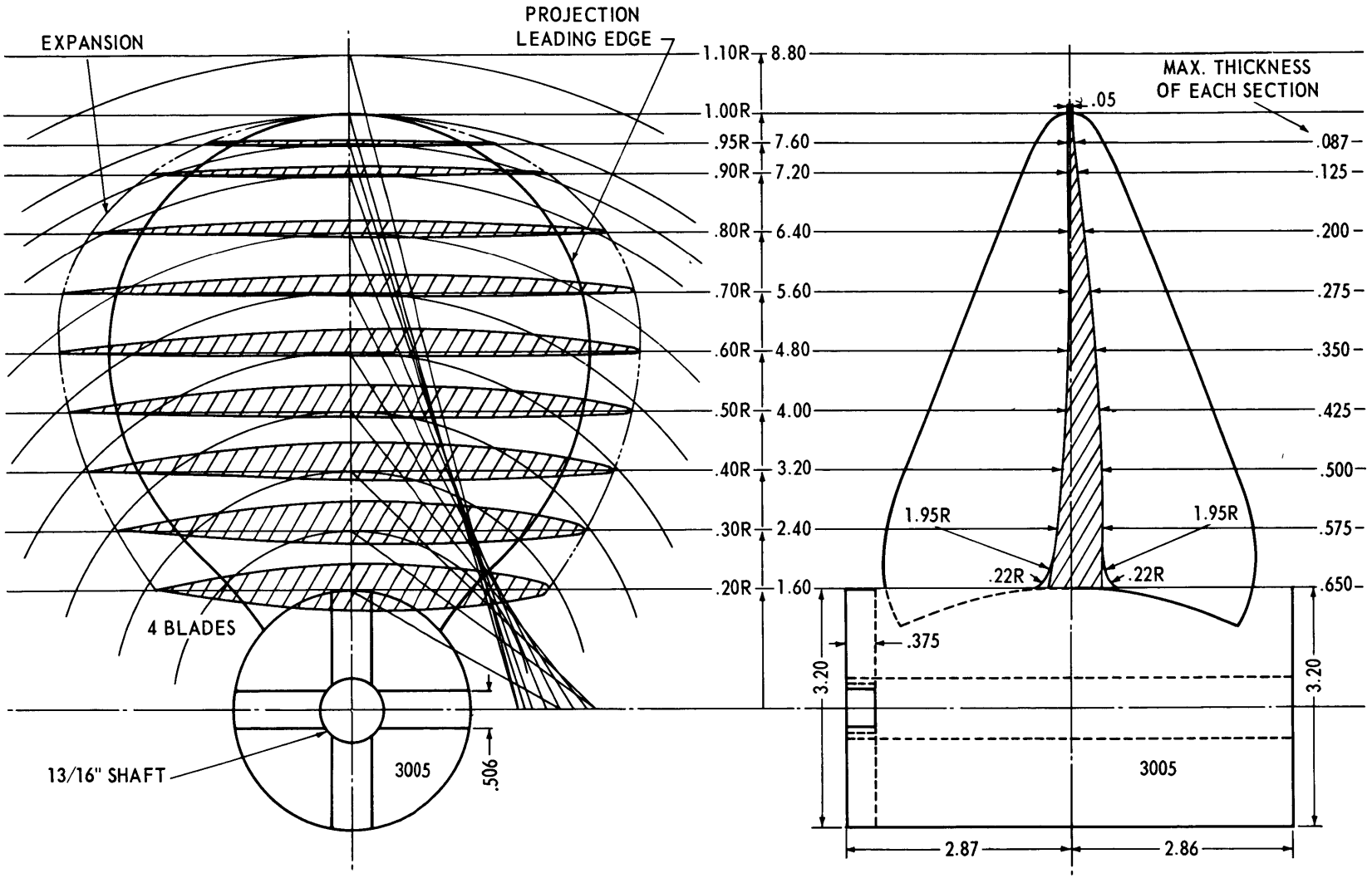

Figure 1 - Destroyer Propeller

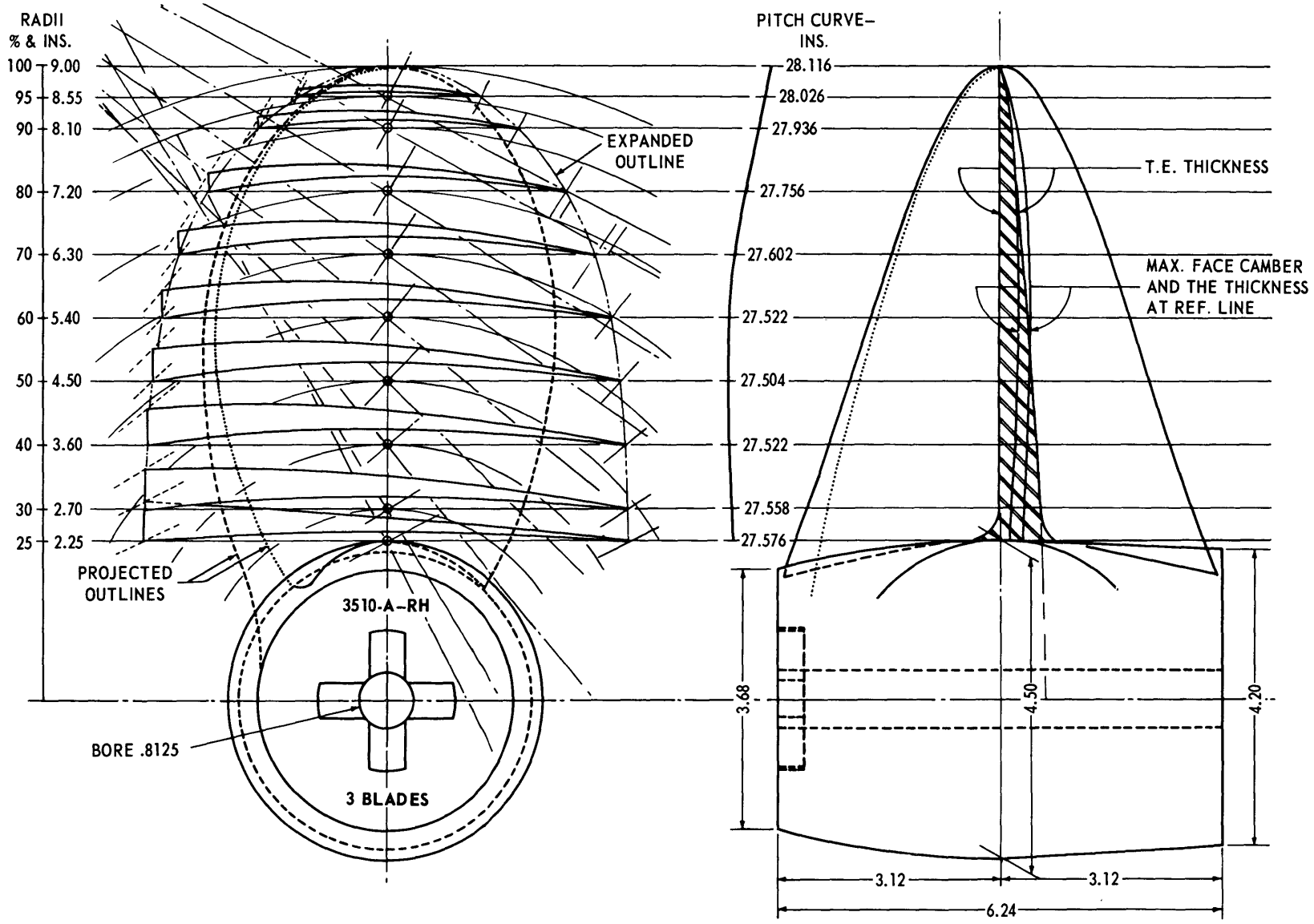

Figure 2 - Supercavitating Propeller

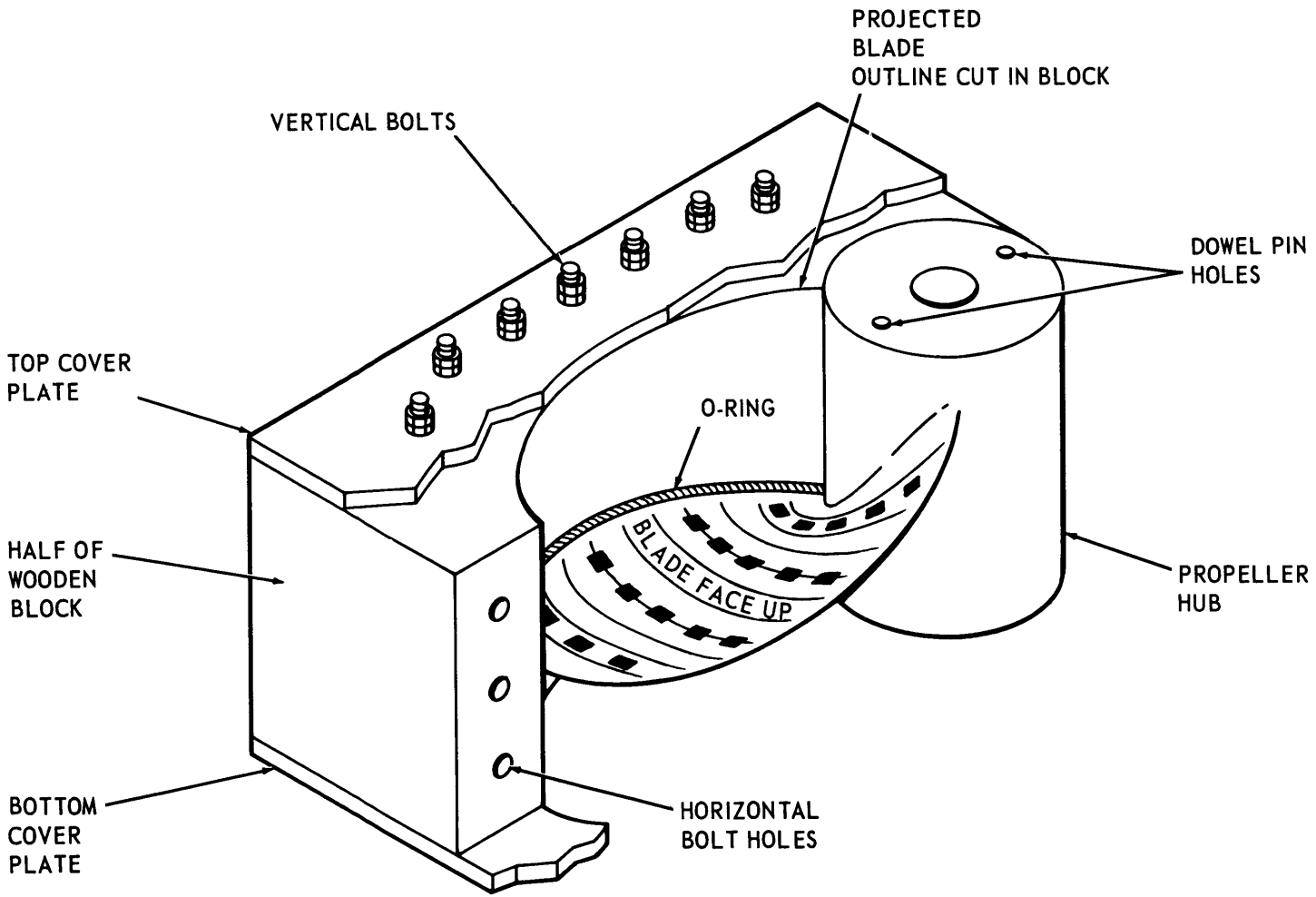

Figure 3 - Cutaway View of Pressure Rig

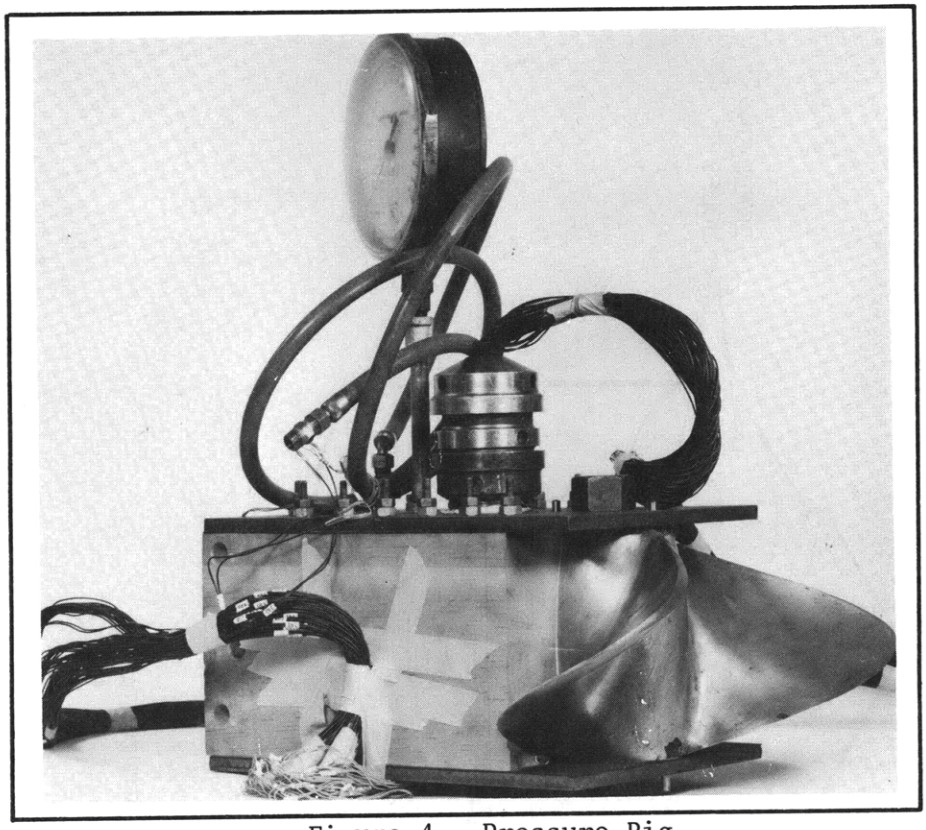

Figure 4 - Pressure Rig

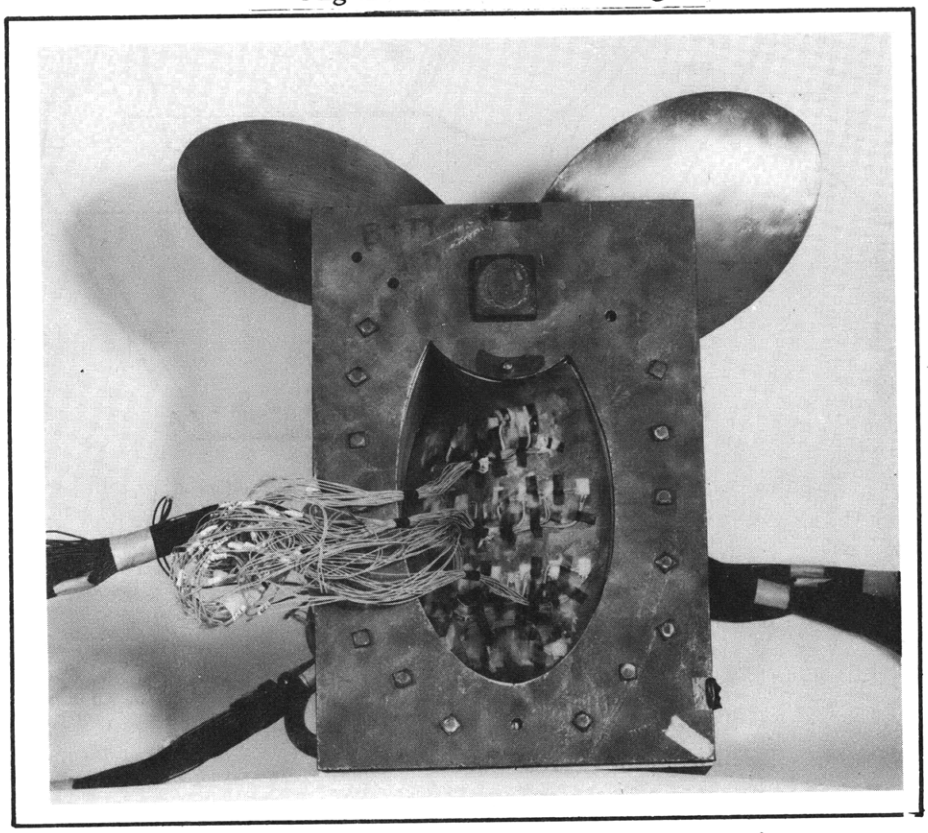

Figure 5 - Underside of Pressure Rig

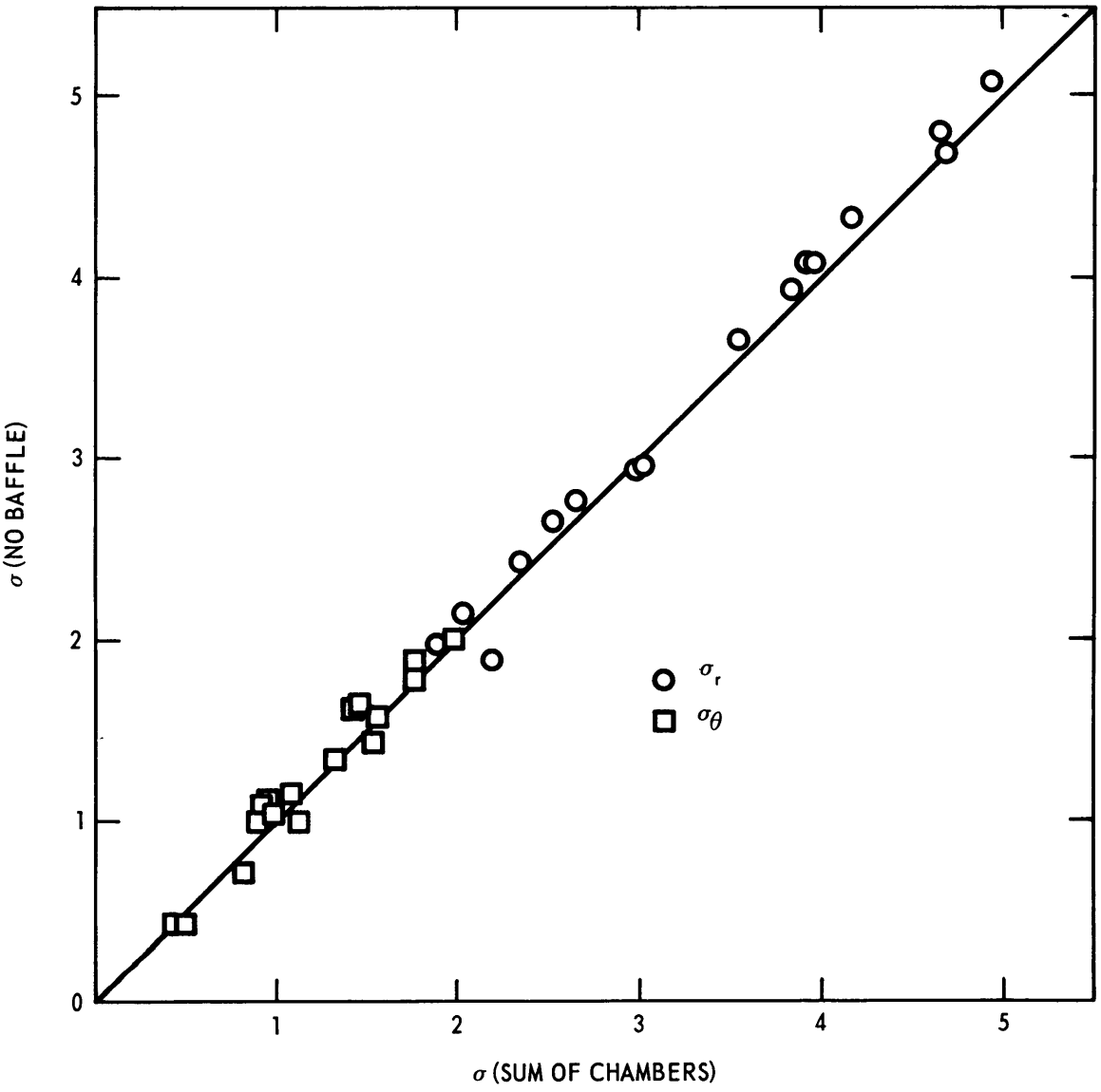

Figure 6 - Comparison of Destroyer-Blade Stresses for Uniform Pressure, Obtained by One- and Two-Chamber Methods

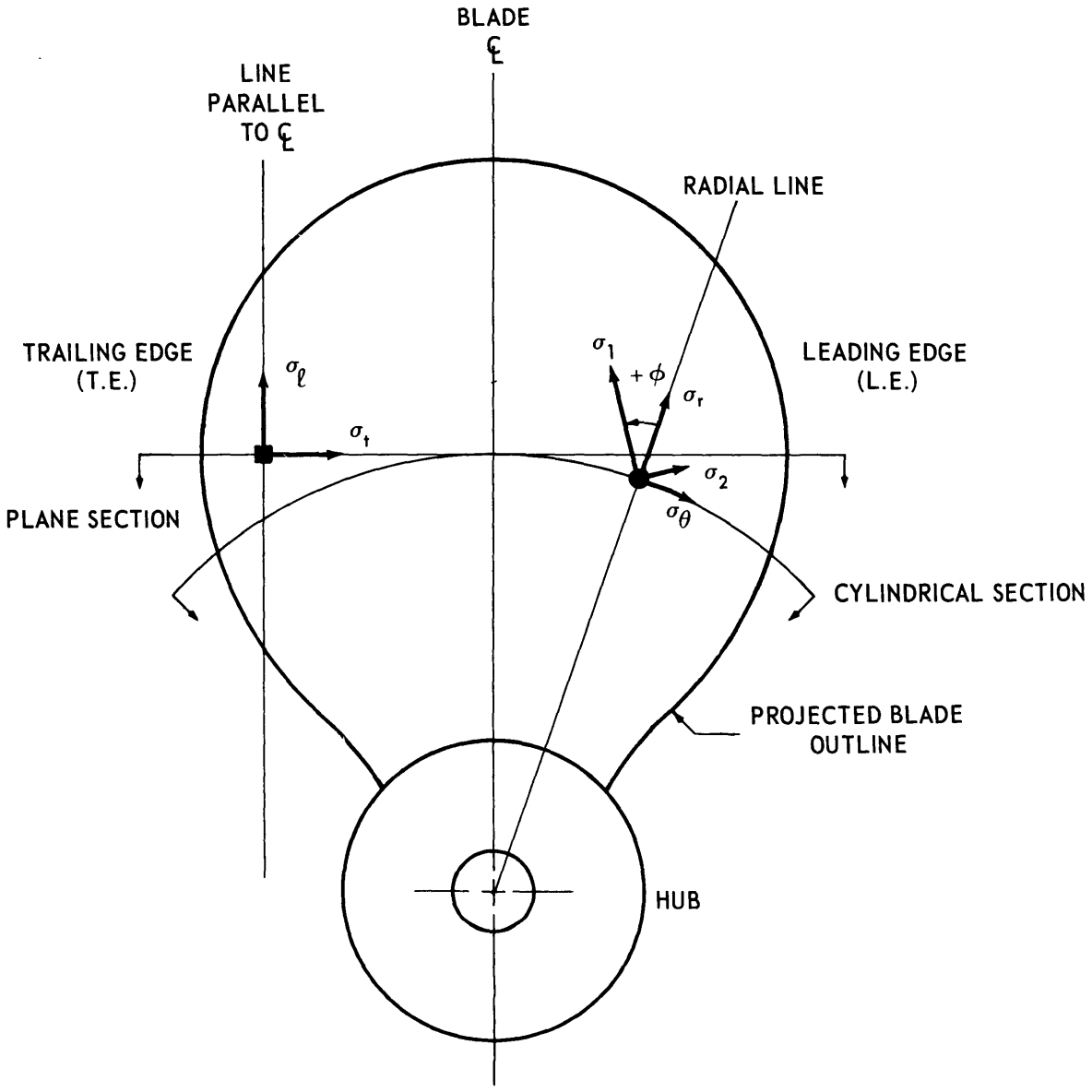

PLANE SECTIONS: σ_ℓ, σ_t . . . LONGITUDINAL AND TRANSVERSE STRESSES

CYLINDRICAL SECTIONS: σ_r, σ_θ . . . RADIAL AND CIRCUMFERENTIAL STRESSES

σ_1, σ_2 . . . MAXIMUM AND MINIMUM PRINCIPAL STRESSES

ϕ . . . ANGLE BETWEEN σ_1 and σ_r, POSITIVE TOWARDS T.E.

Figure 7 - Stress Conventions for Gages, Located on Plane and Cylindrical Blade Sections

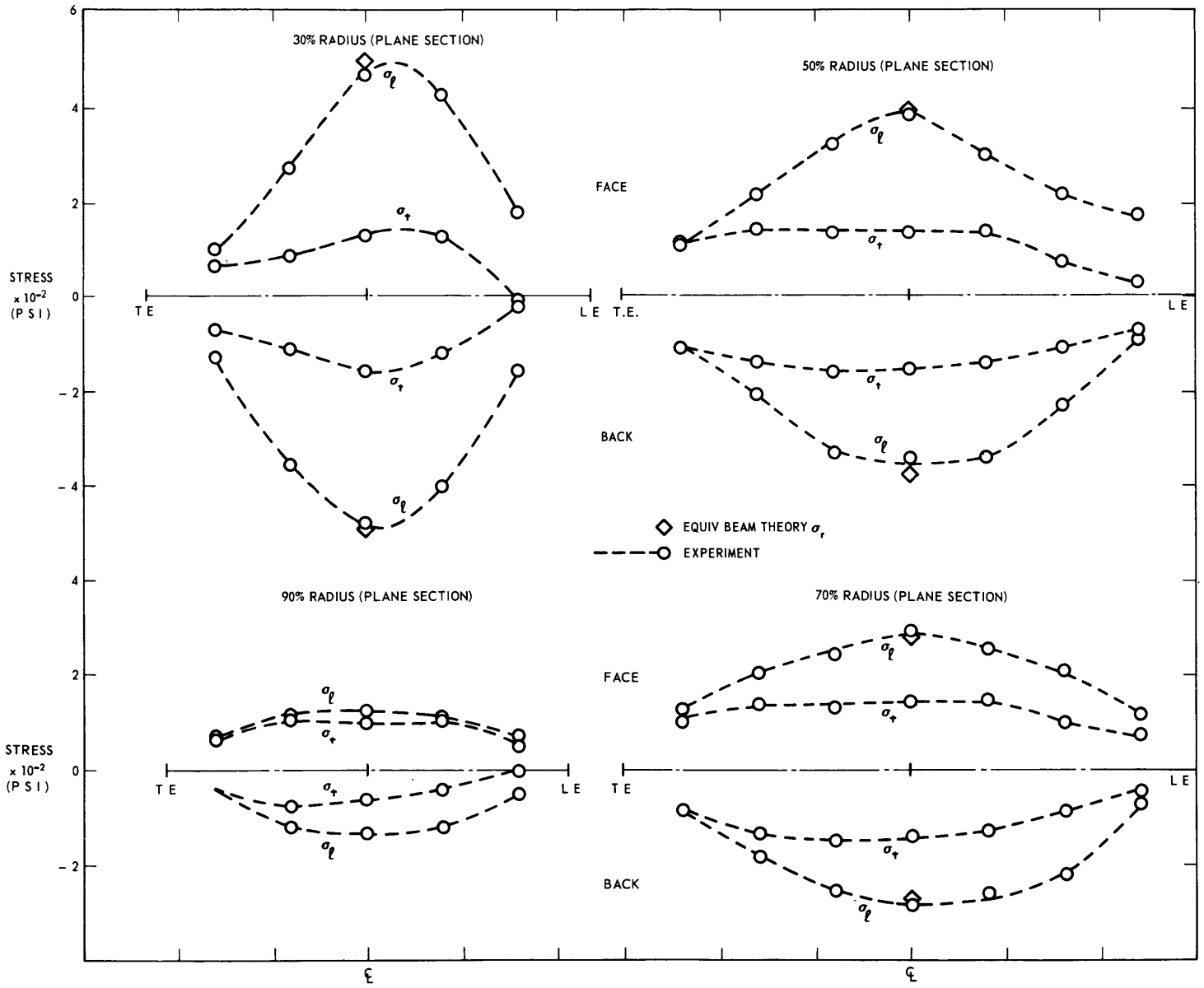

Figure 8 - Destroyer-Blade Stresses on Plane Sections for Uniform Pressure

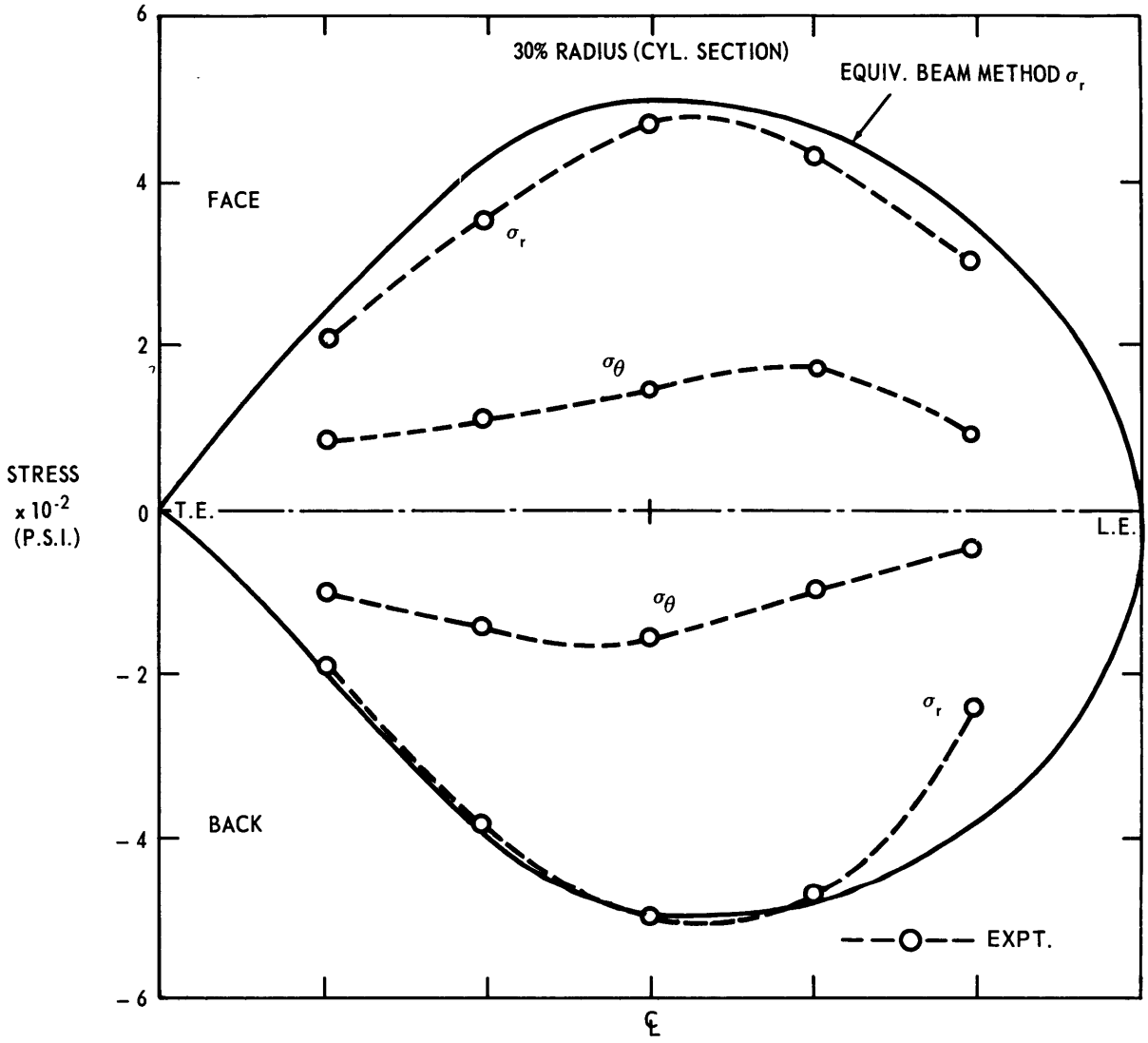

Figure 9 - Comparison of Destroyer-Blade Stresses near Root with Equivalent-Beam Prediction for Uniform Pressure

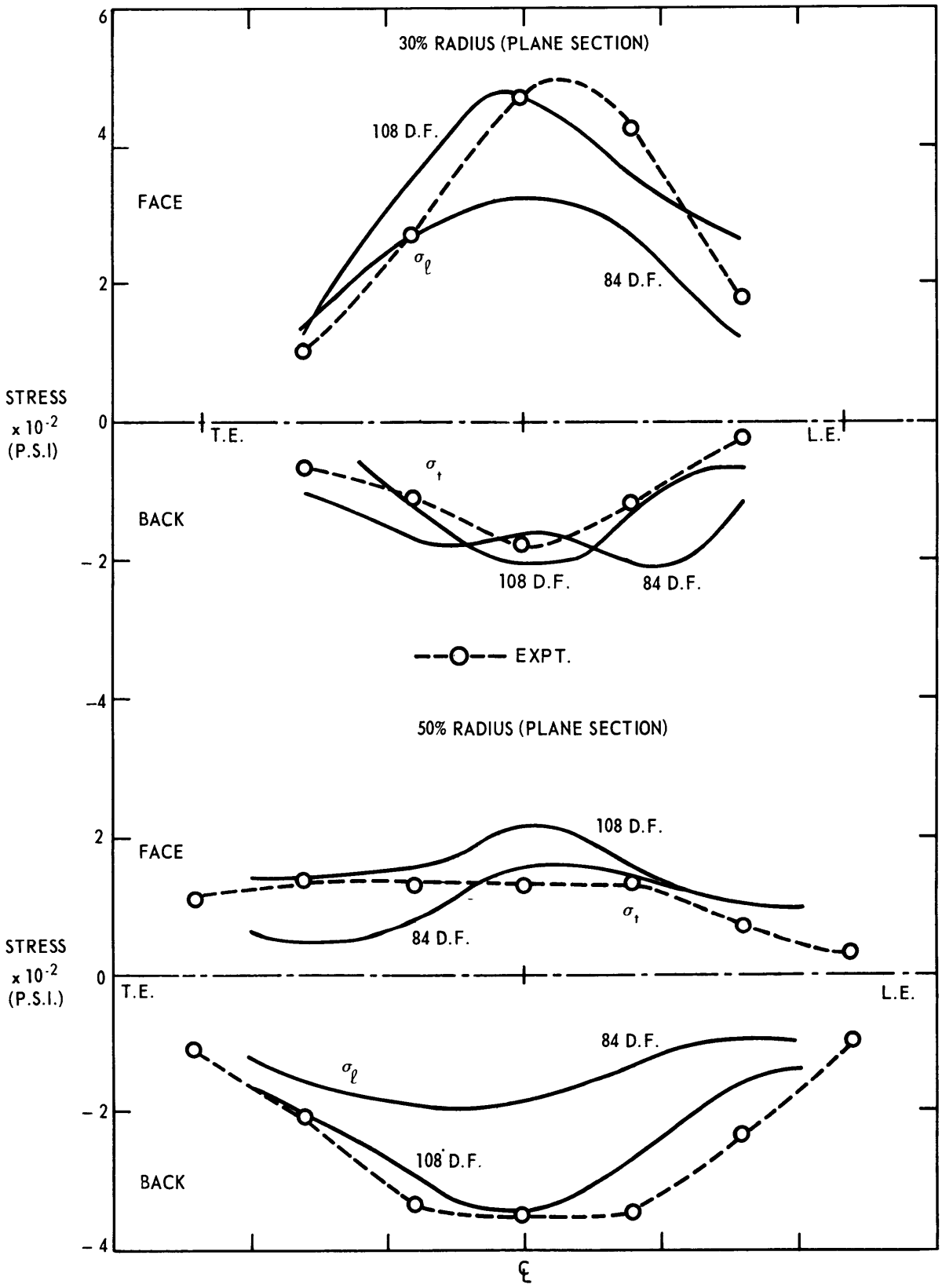

Figure 10 - Comparison of Destroyer Blade Stresses with Shell-Analysis Predictions for Uniform Pressure

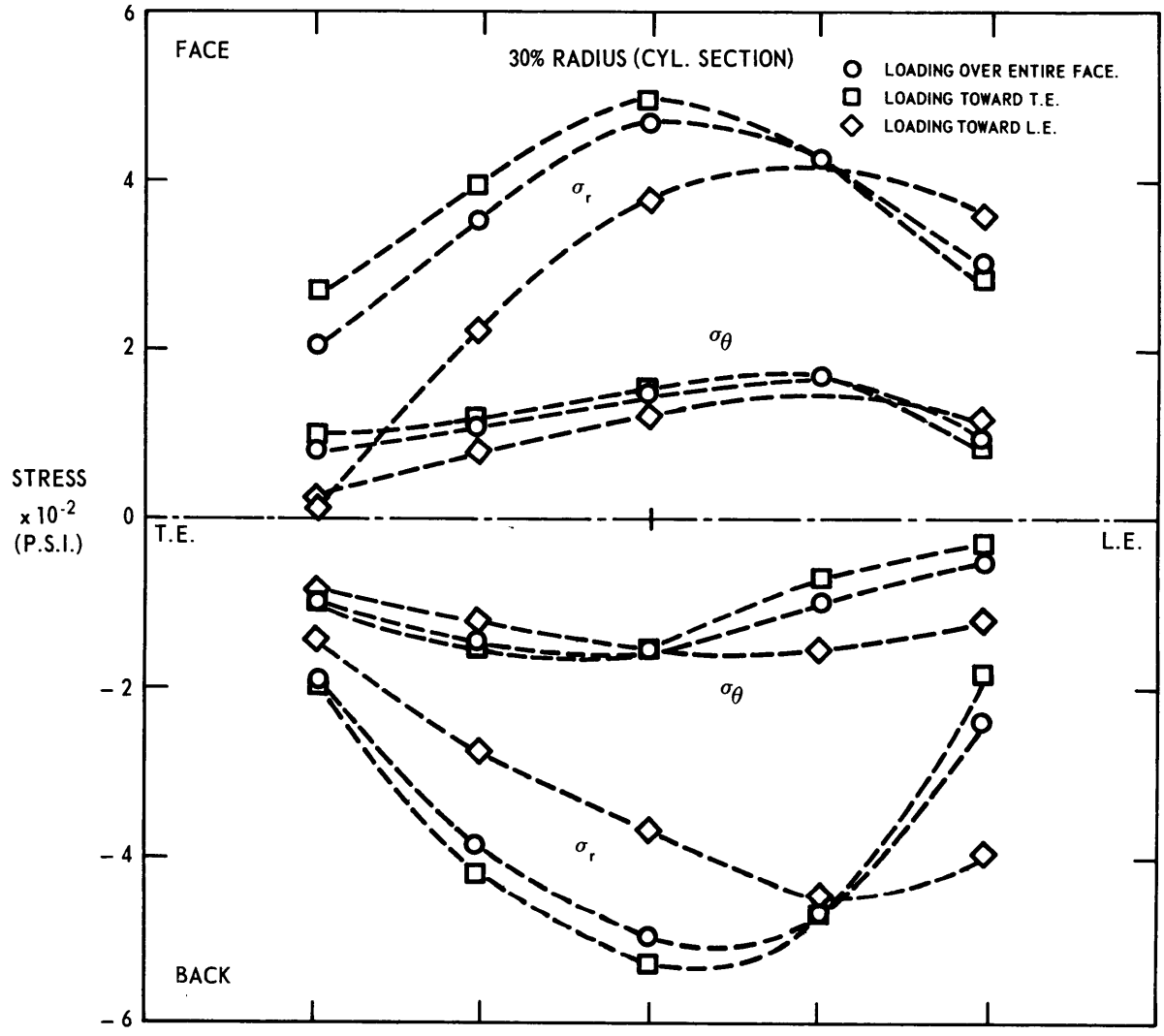

Figure 11 - Destroyer-Blade Stresses near Root for Nonuniform-Pressure Distributions

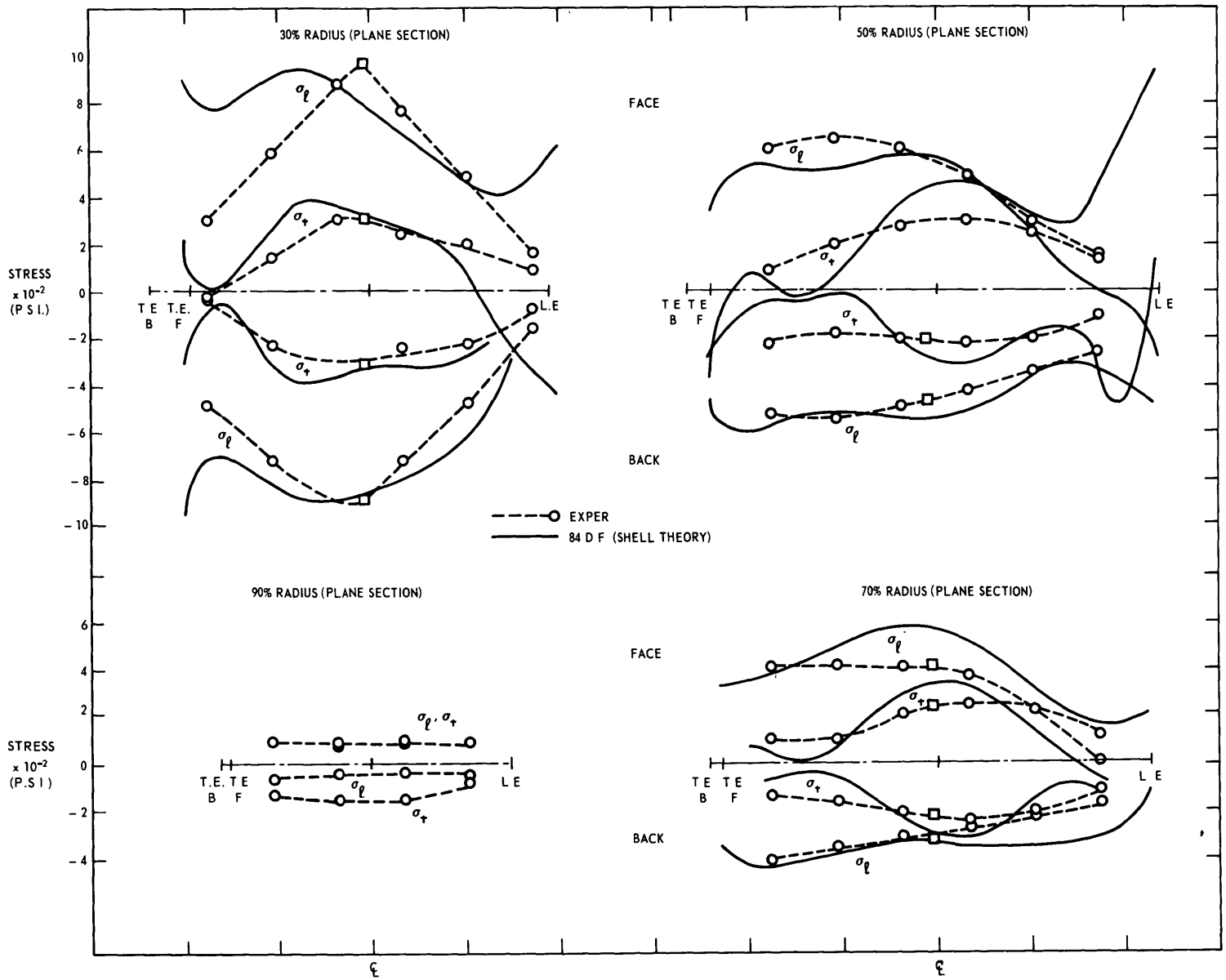

Figure 12 - Supercavitating-Blade Stresses on Plane Sections for Uniform Pressure

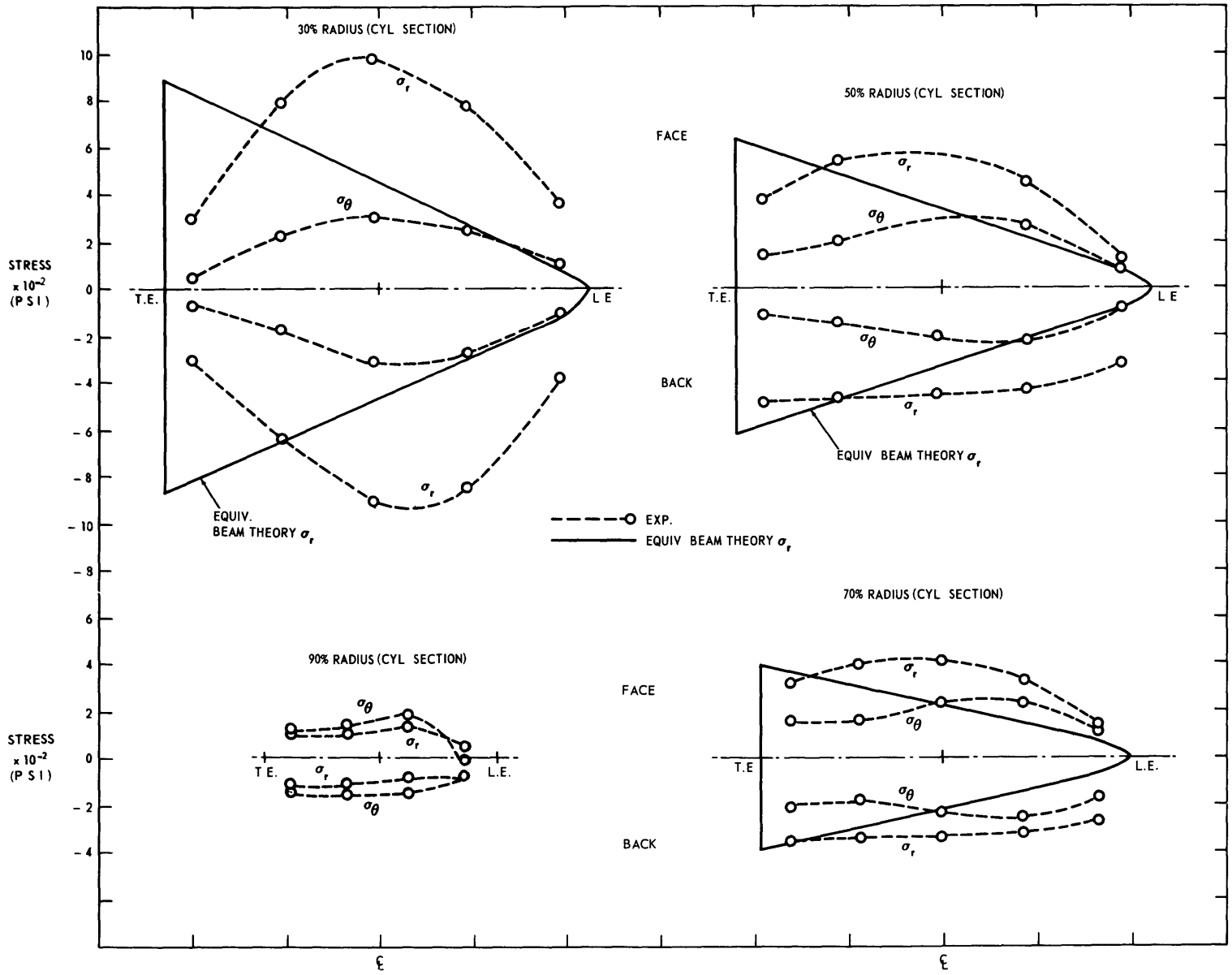

Figure 13 - Supercavitating-Blade Stresses on Cylindrical Sections for Uniform Pressure

TABLE 1

Comparison of Propeller Studies

	Conolly[1]	Davis and English[3]	Terletsky[4]	Antonides[5]	Biezeno[7]	Wereldsma[9]	Shipbuilding Research Association Japan[10]	Present Study	
								Destroyer Propeller	Supercavitating Propeller
Number of Blades	3	4	3	4	4	4	4	4	3
Pitch/Diameter	0.96	1.37	1.20	1.04	0.77	0.77	0.63	1.05	1.53
Blade-Aspect Ratio*	0.82	0.91	0.64	1.25	2.50	1.90	1.64	1.02	1.21
Expanded-Area Ratio	0.81	0.59	0.95	0.64	0.38	0.44	0.50	0.80	0.44
Blade Section	Segmental	Wedge (with annex)	Segmental	Aerofoil	Aerofoil	Aerofoil	Aerofoil	Aerofoil	Wedge
Skew	None	Slight	None	Slight	None	Slight	Slight	None	None
Rake in degrees	None	5	None	None	None	4.5	10.3	None	None
Laboratory Test	Yes	Yes	Yes	No	Yes	Yes	Yes	Yes	Yes
Shipboard Test	Yes	No	No	Yes	No	Yes	Yes	No	No

*Based on mean chord length.

TABLE 2

Principal Stresses of Destroyer-Blade Face at 30-Percent Radius

Percent of Chord from Leading Edge	17			50			67			83		
Formulas	$\frac{\sigma_1}{\sigma_r}$	ϕ deg	$\frac{\sigma_2}{\sigma_\theta}$	$\frac{\sigma_1}{\sigma_r}$	ϕ deg	$\frac{\sigma_2}{\sigma_\theta}$	$\frac{\sigma_1}{\sigma_r}$	ϕ deg	$\frac{\sigma_2}{\sigma_\theta}$	$\frac{\sigma_1}{\sigma_r}$	ϕ deg	$\frac{\sigma_2}{\sigma_\theta}$
Pressure over Entire Blade	1.01	+ 8	0.96	1.00	0	1.00	1.01	- 6	0.95	1.02	-10	0.94
Pressure over Aft Three-Quarters of Blade	1.04	+12	0.87	1.01	+2	0.99	1.00	- 4	0.97	1.02	- 9	0.96
Pressure over Forward One-Quarter of Blade	1.01	- 4	0.97	1.02	-7	0.95	1.09	-17	0.81	3.57	-22	0.18

TABLE 3
Principal Stresses of Supercavitating Blade

Formulas	$\frac{\sigma_1}{\sigma_r}$	ϕ deg	$\frac{\sigma_2}{\sigma_\theta}$	$\frac{\sigma_1}{\sigma_r}$	ϕ deg	$\frac{\sigma_2}{\sigma_\theta}$	$\frac{\sigma_1}{\sigma_r}$	ϕ deg	$\frac{\sigma_2}{\sigma_\theta}$	$\frac{\sigma_1}{\sigma_r}$	ϕ deg	$\frac{\sigma_2}{\sigma_\theta}$	$\frac{\sigma_1}{\sigma_r}$	ϕ deg	$\frac{\sigma_2}{\sigma_\theta}$
Thirty Percent Radius															
Percent of Chord from Leading Edge		7			29			51			73			94	
Face	1.00	- 2	0.97	1.00	- 1	1.00	1.00	0	1.00	1.00	- 7	0.96	1.11	-19	0.29
Back	1.00	+ 1	1.00	1.00	+ 1	1.00	1.00	- 1	1.00	1.00	+ 3	1.00	1.14	-21	0.39
Fifty Percent Radius															
Percent of Chord from Leading Edge		8			30			53			76			94	
Face	1.24	-32	0.61	1.07	-16	0.88				1.23	-27	0.38	1.39	-31	-0.05
Back	1.01	- 5	0.98	1.17	-14	0.92	1.16	-26	0.70	1.20	-26	0.35	1.21	-25	0.10
Seventy Percent Radius															
Percent of Chord from Leading Edge		9			29			51			73			92	
Face	2.74	-48	-0.33	1.34	-36	0.51	1.30	-33	0.46	1.29	-30	0.27	1.46	-34	-0.07
Back	1.00	- 3	1.00	1.24	-37	0.70	1.34	-36	0.51	1.45	-35	0.17	1.55	-37	0.09
Ninety Percent Radius															
Percent of Chord from Leading Edge		13			38			65			89				
Face	2.00	-34	0.50	2.48	-50	0.03	2.43	-49	-0.08	2.34	-48	-0.05			
Back	1.26	-64	0.94	3.10	-51	-0.13	2.63	-41	-0.15	2.38	-49	-0.03			

APPENDIX

PROPELLER OFFSETS

16-Inch Destroyer-Propeller (P-3005)			
X (Fraction of Tip Radius)	Radius--Inches	Chord--Inches	Pitch--Inches
0.20	1.6	5.09	16.80
0.30	2.4	6.03	19.68
0.40	3.2	6.75	19.68
0.50	4.0	7.24	19.04
0.60	4.8	7.43	17.92
0.70	5.6	7.27	16.80
0.80	6.4	6.61	15.68
0.90	7.2	5.15	14.56
1.00	8.0	0	13.44

Offsets from Pitch Line--Inches								
	X = 0.30		X = 0.50		X = 0.70		X = 0.90	
Percent of Chord from Leading Edge	Face	Back	Face	Back	Face	Back	Face	Back
0	0	0	0	0	0	0	0	0
5	-0.088	0.157	-0.046	0.139	-0.030	0.093	-0.021	0.041
10	-0.113	0.226	-0.051	0.202	-0.032	0.135	-0.024	0.057
20	-0.142	0.316	-0.053	0.287	-0.031	0.190	-0.026	0.077
30	-0.159	0.372	-0.054	0.339	-0.031	0.224	-0.028	0.089
40	-0.166	0.401	-0.053	0.367	-0.029	0.243	-0.028	0.096
50	-0.166	0.408	-0.050	0.374	-0.027	0.247	-0.027	0.097
60	-0.151	0.386	-0.042	0.356	-0.022	0.236	-0.025	0.093
70	-0.114	0.327	-0.021	0.306	-0.010	0.204	-0.019	0.081
80	-0.061	0.235	0.006	0.228	-0.006	0.153	-0.011	0.061
90	-0.020	0.133	0.017	0.134	0.011	0.092	-0.006	0.039
95	-0.005	0.074	0.015	0.078	0.008	0.055	-0.006	0.026
100	-0.003	0.003	-0.003	0.003	-0.003	0.003	-0.003	0.003

18-Inch Supercavitating Propeller (P-3604)			
X (Fraction of Tip Radius)	Radius--Inches	Chord--Inches	Pitch--Inches
0.25	2.25	6.84	27.58
0.30	2.70	6.84	27.56
0.40	3.60	6.75	27.52
0.50	4.50	6.61	27.50
0.60	5.40	6.34	27.52
0.70	6.30	5.89	27.60
0.80	7.20	5.06	27.76
0.90	8.10	3.71	27.94
1.00	9.00	0	28.12

Offsets from Pitch Line--Inches								
	X = 0.30		X = 0.50		X = 0.70		X = 0.90	
Percent of Chord from Leading Edge	Face	Back	Face	Back	Face	Back	Face	Back
0	0	0	0	0	0	0	0	0
5	0.025	0.082	0.038	0.087	0.038	0.084	0.022	0.049
10	0.051	0.135	0.078	0.149	0.078	0.139	0.044	0.080
20	0.100	0.237	0.152	0.268	0.151	0.243	0.086	0.140
30	0.138	0.328	0.211	0.371	0.209	0.331	0.119	0.191
40	0.164	0.408	0.251	0.456	0.248	0.401	0.141	0.231
50	0.176	0.474	0.269	0.518	0.266	0.450	0.152	0.260
60	0.173	0.525	0.265	0.559	0.262	0.475	0.149	0.273
70	0.154	0.560	0.236	0.576	0.234	0.478	0.133	0.277
80	0.120	0.580	0.183	0.567	0.181	0.456	0.103	0.256
90	0.069	0.582	0.105	0.534	0.104	0.410	0.059	0.216
95	0.036	0.576	0.056	0.508	0.055	0.373	0.031	0.192
100	0	0.568	0	0.475	0	0.335	0	0.155

REFERENCES

1. Conolly, J.E., "Strength of Propellers," Transactions, Royal Institution of Naval Architects, v. 103 (1960).

2. Morita, S., "Model Propeller Blade Structure Test to Determine Optimum Sweepback Angle," and "Full Scale Supercavitating Propeller Blade Structure Test," Dehavilland Aircraft of Canada, Ltd., Reports HF 1-S-G-3/1 and HF 1-S-G-3/2 (1966).

3. Davis, B.V. and English, J.W., "The Evaluation of a Fully Cavitating Propeller for a High-Speed Hydrofoil Ship," Seventh Symposium on Naval Hydrodynamics, Rome, Italy (1968).

4. Terletsky, B.M., "Stress Measurements on the Propeller Model Blades," Proceedings of 11th International Towing Tank Conference, Tokyo, Japan (1966).

5. Antonides, G., "Propeller Stress Trials on USS FRANKLIN D. ROOSEVELT (CVA-42)," NSRDC Report 2562 (1968).

6. Rosingh, W.H., "Hoogbelaste Scheepschroeven Spanningsberekeningen en Sterktberekening," Schip en Werf, v. 11 (1944) and v. 12 (1945).

7. Biezeno, G.G., "De Experimentele Bepaling van de in een Scheepschroef Optredende Spanningen," De Ingenieur, v. 57 (1945).

8. Romson, J.A., "Sterkteberekening van Scheepsschroeven," Schip en Werf, v. 18 (1951).

9. Wereldsma, R., "Full-Scale Stress Measurements on a Propeller Blade of a 42,000-Ton Tanker," Association Technique Maritime et Aeronautique, Paris (1963), and "Stress Measurements on a Propeller Model for a 42,000 D.W.T. Tanker," International Shipbuilding Progress, v. 12, No. 133 (1965).

10. Shipbuilding Research Association of Japan, "Study of Measuring the Propeller Blade Strength," Report 28, Tokyo, Japan (1959).

11. Taylor, D.W., "The Speed and Power of Ships," Ransdell, Inc., Washington (1933). (First edition published in 1910.)

12. Rosingh, W.H., "Design and Strength Calculations for Heavily Loaded Propellers," Schip en Werf (1937).

13. Hancock, N., "Blade Thickness of Wide-Bladed Propellers," Transactions, Institution of Naval Architects, v. 84 (1942).

14. Cohen, J.W., "On Stress Calculations in Helicoidal Shells and Propeller Blades," Netherlands Research Center T.N.O. for Shipbuilding and Navigation, Report 21S (1955).

15. Venning, E. and Reynolds, T.E., "Analysis and Investigation of Propeller Blade Stress," David Taylor Model Basin Report 1531 (1961).

16. Lieberman, E., "Propeller Blade Vibration and Stress Analysis," General Applied Science Laboratories, Report 283 (1963), and "Extension of Propeller Blade Stress Program," General Applied Science Laboratories, Report 466 (1964).

17. Lane, F., "A Shell Analysis of Propeller Blade Vibration," General Applied Science Laboratories, Interim Scientific Report 1 (1959).

18. Schoenherr, K.E., "Formulation of Propeller Blade Strength," Transactions, Society of Naval Architects and Marine Engineers, v. 71 (1963).

INITIAL DISTRIBUTION

Copies	
4	NAVSHIPS 3 SHIPS 2052 1 SHIPS 033
8	NAVSEC 1 SEC 6100 2 SEC 6110 1 SEC 6140 2 SEC 6144 2 SEC 6148
3	CHBUWEPS 2 Tech Lib (Code DLI-3) 1 Code RUAW-3
3	CHONR 2 Fluid Dyn (Code 438) 1 Sys & Res Gp (Code 492)
1	NUWC, Pasadena
1	NWC, China Lake
1	CDR, USNOL, White Oak
1	DIR, USNRL, Washington
1	ONR, SANFRAN
1	ONR, Boston
1	ONR, Pasadena
1	ONR, Chicago
1	ONR, London
1	NAVSHIPYD PTSMTH Attn: Planning Dept
1	NAVSHIPYD BSN Attn: Planning Dept
1	NAVSHIPYD PEARL Attn: Planning Dept
1	NAVSHIPYD VJO
1	NAVSHIPYD BREM Attn: Planning Dept
1	NAVSHIPYD PHILA Attn: Planning Dept
1	NAVSHIPYD NORVA Attn: Planning Dept
1	NAVSHIPYD CHASN Attn: Planning Dept

Copies	
1	NAVSHIPYD LBEACH Attn: Planning Dept
1	NWL Dahlgren Attn: Computation & Exterior Ballistics Lab
1	CO NROTC & NAVADMY MIT
1	USNA
1	NASL Attn: Lib
1	NAVORDSYSCOM Attn: Code ORD-0541
1	NAVUWRES
1	USL
1	NELC
1	NAVCIVENGLAB
1	NNSB&DDCO Engr Tech Dept
1	NPGSCOL, Monterey
1	NAVFAC
20	DDC
2	NASA 1 Attn: Dr. W.L. Haberman (Code MTY) 1 Attn: Dir of Research (Code RR)
2	ADMIN, MARAD 1 Attn: Ship Div 1 Attn: Coordinator of Research
1	Library of Congress Washington, D.C.
1	Superintendent U.S. MMA, Kings Point
1	Commandant, USCOGARD Attn: Ship Construction Comm
1	Commander, U.S. Army Transportation Research & Development Command Transportation Corps Fort Eustis, Va Attn: Marine Trans Div

Copies	
1	Air Force Office of Sci Res Mechanics Div Washington, D.C.
1	Wright Air Development Div Aircraft Lab W-PAFB, Dayton, Ohio
1	Director Engineering Sci Div Nat'l Sci Foundation Washington, D.C.
1	ORL, Penn State
1	Head, Dept NAME MIT, Cambridge, Mass
1	Univ of Michigan Head, Dept NAME Ann Arbor, Michigan
2	Webb Institute of Naval Architecture Glen Cove, L.I., New York 1 Attn: Lib 1 Adm. Brockett
2	Univ of Calif Berkeley, Calif 1 Attn: Lib 1 Attn: Head, Dept NAVARCH
2	Davidson Lab, SIT Hoboken, N.J. 1 Attn: Director 1 Attn: Dr. S. Tsakonas
1	Puget Sound Bridge & Drydock Seattle, Washington
1	ITEK Corp Vidya Div Palo Alto, Calif
1	TRG, Incorp Melville, N.Y.
1	Lockheed Missiles & Space Co Sunnyvale, Calif Attn: Dept 5701
1	Lockheed Missiles & Space Co Palo Alto, Calif Attn: Tech Info Center
1	Electric Boat Co General Dynamics Corp Groton, Conn
1	Robert Taggart, Inc Fairfax, Va
1	Oceanics, Incorporated Plainview, L.I., N.Y.
1	Gibbs & Cox
1	George C. Sharp, Inc.
1	Grumman Aircraft Corp Bethpage, L.I., N.Y.
1	Hydronautics, Inc.
1	Martin Co Baltimore, Md
1	Boeing Aircraft Corp Advanced Marine Systems Div Seattle, Wash
1	United Aircraft Co Hamilton Standard Div Windsor Locks, Conn.
1	AVCO Inc. Lycoming Div Washington, D.C.
2	General Dynamics - Convair San Diego, Calif 1 Attn: Dr. B.R. Parkin 1 Attn: Chief of ASW/Marine Sciences
1	SNAME
1	ASNE, Washington
1	ASME Research Committee in Information New York, N.Y.
1	General Applied Sci Labs Westbury, New York Attn: E. Lieberman

UNCLASSIFIED
Security Classification

DOCUMENT CONTROL DATA - R & D

(Security classification of title, body of abstract and indexing annotation must be entered when the overall report is classified)

1 ORIGINATING ACTIVITY (Corporate author)	2a. REPORT SECURITY CLASSIFICATION
Naval Ship Research and Development Center Washington, D.C. 20007	UNCLASSIFIED
	2b. GROUP

3. REPORT TITLE

STATIC STRESSES ON WIDE-BLADED PROPELLERS

4 DESCRIPTIVE NOTES (Type of report and inclusive dates)

Final Report

5 AUTHOR(S) (First name, middle initial, last name)

Justin H. McCarthy and Joseph S. Brock

6. REPORT DATE	7a. TOTAL NO. OF PAGES	7b. NO. OF REFS
February 1970	35	18

8a. CONTRACT OR GRANT NO.	9a. ORIGINATOR'S REPORT NUMBER(S)
b. PROJECT NO. Subproject S-R009 01 01	3182
c. Task 103	9b. OTHER REPORT NO(S) (Any other numbers that may be assigned this report)
d.	AD 704 492

10. DISTRIBUTION STATEMENT

This document has been approved for public release and sale; its distribution is unlimited.

11. SUPPLEMENTARY NOTES	12. SPONSORING MILITARY ACTIVITY
	Naval Ship Systems Command

13. ABSTRACT

Static stresses were obtained in laboratory experiments for a destroyer propeller, having aerofoil blade sections, and a supercavitating propeller, having wedge-shaped blade sections, using specially constructed pressure chambers that allowed the blade faces to be loaded under air pressure. A new method for applying beam theory is presented that closely predicts the magnitude and distribution of radial stresses on the destroyer propeller blade. For the supercavitating propeller, neither the proposed beam-theory method nor a particular computerized-shell analysis can be considered entirely satisfactory for prediction of blade stresses.

14 KEY WORDS	LINK A		LINK B		LINK C	
	ROLE	WT	ROLE	WT	ROLE	WT
Propeller Stress						
Wide-Bladed Propellers						
Supercavitating Propellers						
Static Stress						
Propeller Stress Experiments						
Propeller Stress Calculations						